Magnetic properties of finite Fe chains at fcc Cu(001) and Cu(111) surfaces

B. Lazarovits,[1] L. Szunyogh,[1,2] P. Weinberger,[1] and B. Újfalussy[3]
[1]*Center for Computational Materials Science, Technical University Vienna, A-1060, Gumpendorferstrasse 1.a., Vienna, Austria*
[2]*Department of Theoretical Physics and Center for Applied Mathematics and Computational Physics, Budapest University of Technology and Economics, Budafoki út 8., H-1521 Budapest, Hungary*
[3]*Oak Ridge National Laboratory, Oak Ridge, Tennessee 37831-6114, USA*
(Received 24 February 2003; published 31 July 2003)

We present a systematic study of the magnetic moments and magnetocrystalline anisotropy of finite monoatomic Fe_n $(1 \leqslant n \leqslant 9)$ chains deposited along the $(1\bar{1}0)$ direction on top of fcc Cu(001) and Cu(111) surfaces as well as embedded into the uppermost three surface layers and into a perfect copper bulk host. The calculations are performed fully relativistically using the embedding technique within the Korringa-Kohn-Rostoker method. We focused our investigations on the effect of the interaction between the Fe atoms as well as between the Fe and host atoms on the magnetic properties of the chains. We found that the calculated spin and orbital moments in the Fe chains are systematically larger than in the corresponding monolayer. Exploring the magnetic anisotropy properties of these systems we obtained a strong out-of-plane easy axis for wires deposited both on the Cu(001) and Cu(111) surfaces, while for the embedded chains the orientation of the easy axis depends on the distance from the surface. We also found remarkable anisotropies for two different in-plane magnetic orientations: namely, for the one parallel and the other perpendicular to the chains.

DOI: 10.1103/PhysRevB.68.024433 PACS number(s): 75.30.Hx, 73.22.−f, 75.30.Gw

I. INTRODUCTION

The fast development of manufacturing and observation techniques made available a large number of different geometrical arrangements of magnetic impurities on metallic surfaces like dots, wires, stripes, or corrals. Due to their sensitivity to the local environment, the magnetic properties of transition-metal structures can thus be greatly modulated, exploring a wide spectrum of magnetic phenomena, e.g., increased spin and orbital magnetization and strong magnetic anisotropies as well as a temperature and time dependence of the magnetization. Since the experiments of Elmers *et al.*[1] on Fe nanostripes on a W(110) surface, often referred to as the pioneering work in the field of magnetic nanowires, a large number experimental and theoretical works have been dealing with the electronic and magnetic properties of these (quasi-)one-dimensional systems.[2–10] In particular, the structure and magnetism of monoatomic Fe wires grown on different stepped $Cu(11n)$ $(n=3-11)$ surfaces were investigated by Spišák and Hafner,[11] while Eisenbach *et al.*[12] demonstrated that changing the crystallographic orientation of infinite Fe wires embedded into Cu bulk can even result in a change of the easy axis.

It was also shown by Stepanyuk *et al.*[13] that small magnetic clusters buried by surface layers can be energetically more favorable than deposited on the surface. At an early stage of growth of Fe films on a vicinal Cu(111) surface iron forms a quasi-one-dimensional (quasi-1D) fcc-related structure along the step edges due to the step decoration effect. For the Fe stripes oriented along the (110) axis an easy direction of magnetization pointing perpendicular to the surface and a time- and temperature-dependent magnetization was reported by Shen *et al.*[14,15] Very recently, for the same system Boeglin *et al.*[16] observed an in-plane magnetocrystalline anisotropy energy (MAE) favoring an orientation perpendicular to the chain.

The objective of the recent paper is to study in terms of *fully relativistic*, *ab initio* calculations the magnetic properties of Fe chains deposited along the $(1\bar{1}0)$ direction of Cu(001) and Cu(111) surfaces as well as buried by the surface layers. By performing calculations for different lengths of the chain, $1 \leqslant n \leqslant 9$, and by varying its distance from the surface, we shall emphasize the role of the Fe-Fe and Fe-host interactions on the spin and orbital moments as well as on the MAE. Concomitantly, in terms of the above quantities we also describe the crossover from a pointlike impurity (0D) to a linear chain (1D).

II. THEORETICAL APPROACH

Within multiple-scattering theory, the matrix of the so-called scattering path operator (SPO), $\boldsymbol{\tau}_{\mathcal{C}}$, corresponding to a finite cluster $\mathcal{C}$ embedded into a host system can be obtained from the following Dyson equation:[17]

$$\boldsymbol{\tau}_{\mathcal{C}}(E) = \boldsymbol{\tau}_h(E)\{\boldsymbol{I} - [\boldsymbol{t}_h^{-1}(E) - \boldsymbol{t}_{\mathcal{C}}^{-1}(E)]\boldsymbol{\tau}_h(E)\}^{-1}, \qquad (1)$$

where $\boldsymbol{t}_h(E)$ and $\boldsymbol{\tau}_h(E)$ denote the single-site scattering matrix and the SPO matrix for the unperturbed host confined to the sites in $\mathcal{C}$, respectively, while $\boldsymbol{t}_{\mathcal{C}}$ comprises the single-site scattering matrices of the embedded atoms. Note that Eq. (1) takes into account all scattering events both in and out of the cluster. Once $\boldsymbol{\tau}_{\mathcal{C}}$ is derived, all quantities of interest—i.e., the charge and magnetization densities and the spin and orbital moments as well as the MAE for the cluster—can be calculated.[17]

Self-consistent calculations of the host copper were performed in terms of the fully relativistic screened Korringa-Kohn-Rostoker method[18,19] using 45 and 80 k points in the irreducible segment of the surface Brillouin zone in the case of (001) and (111) surfaces, respectively, and three layers of empty spheres to represent the vacuum region. The cluster

calculations were then carried out such that the Fe atoms substituted sites along the $(1\bar{1}0)$ direction in the first vacuum layer and in the uppermost three surface layers as well as in the perfect 3D bulk host. No attempts were made to include lattice relaxation effects: the host and cluster sites refer therefore to the positions of an ideal fcc parent lattice with the experimental Cu lattice constant. The local spin-density approximation as parametrized by Vosko *et al.*[20] was applied throughout, and the effective potentials and fields were treated within the atomic sphere approximation (ASA). When solving the Kohn-Sham-Dirac equation and also for the multipole expansion of the charge densities, a cutoff of $\ell_{max}=2$ was used.

By using the self-consistent potentials with a magnetization pointing perpendicular to the surface (along the z axis), we calculated the MAE by means of the magnetic force theorem[21–23] as a difference of band energies,[17]

$$\Delta E_{\mu-z}=E_{\mu}^{b}-E_{z}^{b} \quad (\mu=x,y), \tag{2}$$

$$\Delta E_{\mu-z}>0, \quad z \text{ preferred},$$

$$\Delta E_{\mu-z}<0, \quad \mu \text{ preferred}, \tag{3}$$

where the axes x and y refer to in-plane directions parallel and perpendicular to the chains, respectively. Quite naturally, within this formalism, the MAE can be resolved into contributions with respect to atoms. In principle, the magnetic dipole-dipole interaction part of the MAE,[22] $\Delta E_{\mu-z}^{dd}$, should also be considered. Evidently, for the case of $y-z$ this contribution almost vanishes. For the case of $x-z$ we can make an estimate based on the calculations of Ref. 12, which gives $\Delta E_{x-z}^{dd}\sim 0.12$ meV/Fe atom for chains in the bulk and ~ 0.2 meV/Fe atom for chains on top of the surfaces. Since these values are typically by a factor of 3 smaller than the corresponding ΔE_{x-z}^{b} (see, e.g., Fig. 7), in the present study we have not discussed the magnetic dipole-dipole interaction part of the MAE.

III. SPIN AND ORBITAL MOMENTS

For the Cu atoms adjacent the Fe impurities we found a relatively weak magnetic polarization even in the surface layer, where the polarizability of the host atoms is expected to be the strongest. The calculated spin moments of these host atoms (S_z^{Cu}) were about $0.02\mu_B$, and the corresponding orbital moments (L_z^{Cu}) were less than $10^{-3}\mu_B$. These values are much lower than found for substrate Pt atoms in a similar geometrical arrangement with Co chains [$S_z^{Pt}=(0.09–0.14)\mu_B$, $L_z^{Pt}=(0.02–0.04)\mu_B$] (Ref. 24). For the Co-Pt system our tests showed that treating only one shell of host atoms around the impurities self-consistently was sufficient to get reasonable results for the magnetic properties of the impurities. The weaker polarization of the Cu atoms as compared to the Pt atoms implies that this approach applies also for the Cu-Fe system.

In Fig. 1 the spin and orbital moment of a single Fe impurity is shown as a function of the distance of the impurity from the surface. We found that the spin-only magnetic moment of a single Fe impurity deposited on a Cu(001) surface ($3.19\mu_B$) is by about 15% larger than in the corresponding monolayer case ($2.78\mu_B$) (Ref. 25). This result agrees well with the full-charge density calculations of Stepanyuk *et al.*[26]

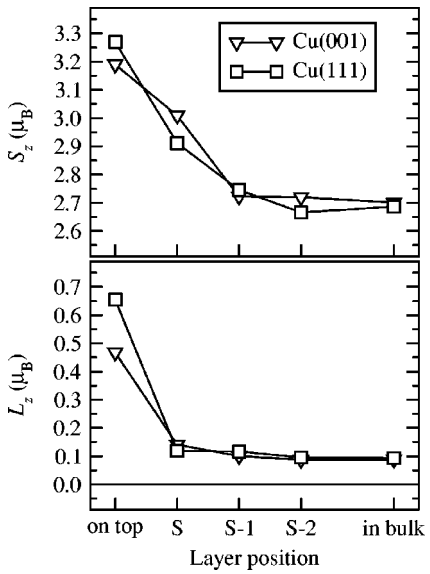

FIG. 1. Calculated spin (S_z) and orbital moments (L_z) of a single Fe impurity embedded at different distances from a Cu(001) and a Cu(111) surface with a magnetization along the surface normal (z). The position of the impurity is labeled as follows: on top, first vacuum layer; S, surface layer; S-1, first subsurface layer; S-2, second subsurface layer; in bulk, perfect bulk host.

A similar comparison between an Fe impurity embedded into the bulk host and an Fe monolayer sandwiched by two semi-infinite Cu(001) substrates shows that the difference between the corresponding spin moments of Fe ($2.70\mu_B$) and ($2.54\mu_B$), respectively, is by about 6% smaller than at the surface. This obviously demonstrates that the Fe-Cu interaction, subject to the actual position of the Fe impurities, plays an important role in the formation of the magnetic properties of the Fe nanostructures.

Placing the Fe impurity at increasing distances from the surface one can selectively trace the effect of hybridization between the impurity and host atoms. We observed a clear-cut correlation between the coordination number N_{Cu} of the impurity formed by the nearest-neighbor Cu atoms and the actual value of the spin moment of the impurity. Inspecting Fig. 1 one can see that the spin moment of the Fe impurity on Cu(111) ($3.27\mu_B$) is larger than that on the Cu(001) surface ($3.19\mu_B$), which can be attributed to the smaller number of nearest-neighbor Cu sites of the Fe impurity in case of a (111) surface ($N_{Cu}=3$) than in case of a (001) surface ($N_{Cu}=4$). For an impurity embedded into the first Cu surface layer, on the contrary, S_z^{Fe} is larger for the (001) surface ($3.01\mu_B$) for which now $N_{Cu}=8$ as compared to the (111) surface layer ($2.91\mu_B$) with $N_{Cu}=9$.

Clearly enough, for Fe impurities buried deeper in the host, S_z^{Fe} differs only very little for the two kinds of surfaces and also it converges rapidly to S_z of an Fe impurity embedded into the bulk ($2.70\mu_B$). The sensitivity of S_z^{Fe} on the choice of the surface and the distance of the impurity from

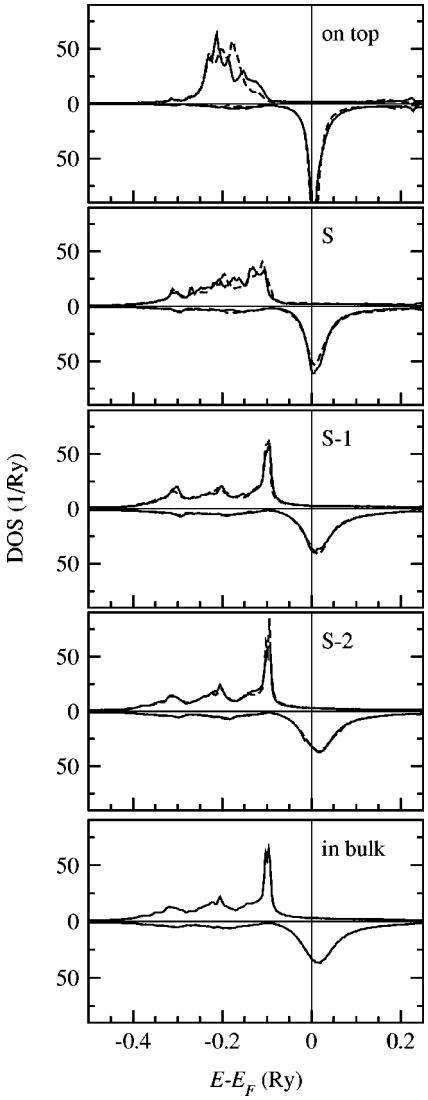

FIG. 2. Calculated spin-projected densities of states (DOS) of an Fe impurity embedded into different layers of the Cu(001) (solid line) and the Cu(111) (dashed line) surfaces and into a Cu bulk host with a magnetization pointing normal to the surface (z). In each entry, the majority- and the minority-spin DOS is depicted in the upper and lower panels, respectively. For the notation of the position of the impurity see Fig. 1.

the surface can be traced in Fig. 2 in terms of spin-projected densities of states (DOS) (Refs. 19 and 27) of the Fe impurity. Note that the DOS was calculated at an energy mesh parallel to the real axis with an imaginary part of 1 mRy. As can be seen the very sharp minority-spin *d* band of the Fe adatoms on the surface is intersected by the Fermi level just a little beneath the maximum of the peak. Therefore, the broadening of the minority-spin band due to the increasing hybridization with Cu pushes more states below the Fermi level than above, resulting into a decrease of the spin moment.

In Figs. 3 and 4 the calculated spin moments are displayed for each Fe atom in the chains near the Cu(001) and Cu(111) surfaces, respectively. As can be seen, independent from the distance from the surface, for longer chains (n

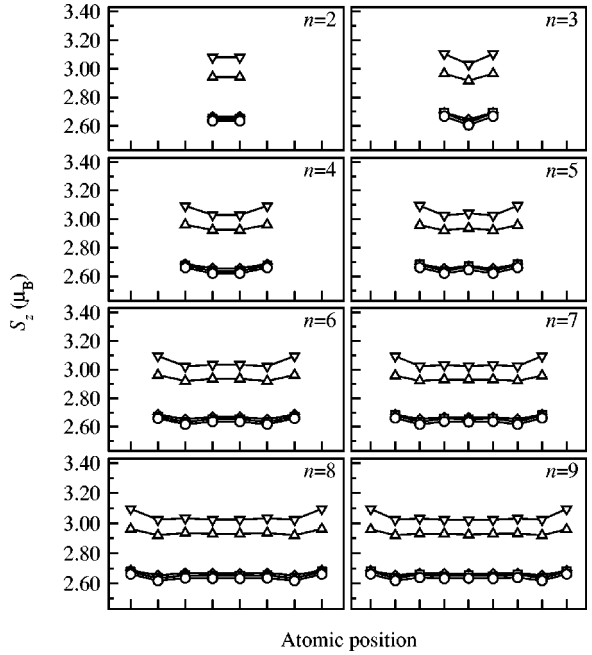

FIG. 3. Calculated spin moments (S_z) of the Fe atoms in Fe_n ($n=2,\ldots,9$) chains at the Cu(001) surface with a magnetization pointing normal to the surface (∇, on top; $\triangle$, layer S; $\diamond$, layer S-1; $\square$, layer S-2; $\bigcirc$, in bulk; see Fig. 1).

$\geqslant 3$), S_z^{Fe} is systematically higher at the edges of the chains than in the middle. This feature can (again) be attributed to the reduced coordination number N_{Fe} formed by the adjacent Fe atoms ($N_{Fe}=2$ and 1 for atoms inside the chain and at the edge, respectively), since the strong Fe-Fe hybridization low-

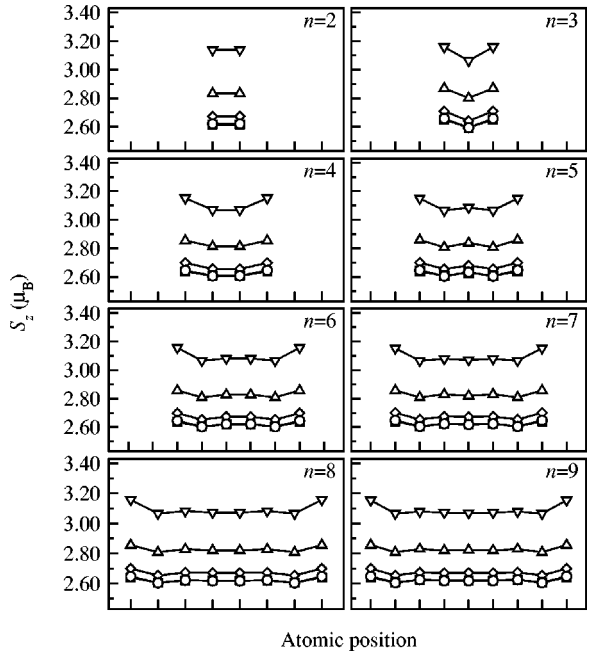

FIG. 4. Calculated spin moments (S_z) of the Fe atoms in Fe_n ($n=2,\ldots,9$) chains at the Cu(111) surface with a magnetization pointing normal to the surface (∇, on top; $\triangle$, layer S; $\diamond$, layer S-1; $\square$, layer S-2; $\bigcirc$, in bulk; see Fig. 1).

ers the spin moment of the Fe atoms. Note that we observed a similar trend for Co chains on Pt(111),[24] while for Rh chains the opposite trend was reported.[6] The extent of the difference between the spin moments of the inner and outermost atoms is slightly affected by the distance from the surface.

For Fe_9 on top of Cu(111) the difference between S_z^{Fe} of the inner atoms ($3.07\mu_B$) and that of the outermost atoms ($3.15\mu_B$) is about 2% while for a chain of the same length embedded into the bulk this difference is only about 1%. In general, it can be concluded that the spin magnetism of the Fe impurities is affected by the Fe-Cu interaction and modulated mainly by the distance of the magnetic nanostructure from the surface and also by the Fe-Fe interaction.

In the lower panel of Fig. 1 one can see that the orbital moment of an Fe impurity dramatically decreases from its value as an adatom when it is placed into the surface and, by further moving below the surface, it slowly tends to the corresponding bulk value. In fact, the orbital moment of the Fe adatom is about 3.3 times larger on top of the (001) surface ($0.47\mu_B$) than in the surface layer ($0.14\mu_B$), while for the (111) surface this ratio is as large as 5.5 ($0.65\mu_B \rightarrow 0.12\mu_B$). Note that these changes are much larger than the corresponding changes in the spin moments [$\sim 6\%$ and $\sim 12\%$ for the (001) and (111) surfaces, respectively].

Similar to our previous studies of atomic-scale magnetic structures,[17,24] this implies that the orbital moment is much more sensitive to the local environment than the spin magnetization: due to the localization of the *d*-like states (see also Fig. 2), L_z^{Fe} is less quenched for the adatom as compared to an impurity in or below the surface. For the same reason, the adatom on a Cu(111) surface carries a considerably higher value of L_z^{Fe} than that deposited on a Cu(001) surface.

The calculated orbital moments of the Fe atoms in the chains are shown in Figs. 5 and 6. As in the case of a single impurity, the chains deposited on the surface display a qualitatively different behavior as compared to those in or below the surface: L_z is much larger and also it exhibits remarkable oscillations for the chains on the surface.

Apparently these features are more pronounced for chains on a (111) surface than the (001). In case of an Fe trimer on Cu(111), e.g., L_z of the outer atoms ($0.35\mu_B$) is about 2.2 times larger than that of the central one ($0.15\mu_B$). For longer chains ($n>7$) the oscillations of L_z inside the chains are clearly damped. From Figs. 5 and 6 a rapid convergence of the orbital moment to the value of the chains embedded into the bulk host can be inferred.

A transition from a pointlike (0D) to a quasi-one-dimensional (1D) system can be traced in terms of the spin and orbital moments of the central atoms of the chains shown in Fig. 7 as a function of the length of the chains, *n*. As also can be inferred from Figs. 1, 3, 4, 5, and 6, up to $n=3$ the magnetic moments decrease systematically and then seem to converge to a well-defined value. The value of S_z^{Fe} and L_z^{Fe} extrapolated from the data in Fig. 7 numerically to $n=\infty$, listed in Table I, can be interpreted as an estimation for the moments in the corresponding infinite chains.

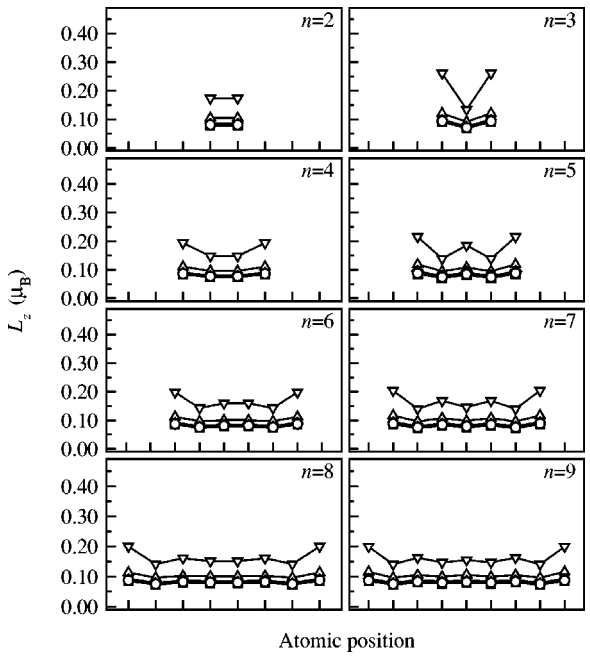

FIG. 5. Calculated orbital moments (L_z) of the Fe atoms in Fe_n ($n=2,\ldots,9$) chains at the Cu(001) surface with a magnetization pointing normal to the surface (∇, on top; $\triangle$, layer S; $\diamond$, layer S-1; $\square$, layer S-2; $\bigcirc$, in bulk; see Fig. 1).

These estimated values for S_z^{Fe} compare well with the theoretical results for infinite Fe wires at a Cu(117) surface, $2.86\mu_B$–$2.96\mu_B$ depending an the actual position of the wire,[11] and to that embedded into a copper bulk host, $S_z^{Fe}=2.50\mu_B$ (Ref. 12). Also listed are in Table I the moments of

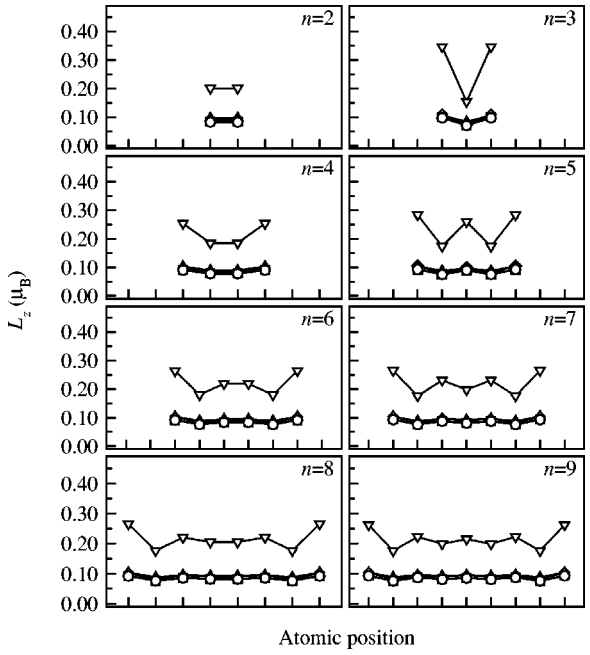

FIG. 6. Calculated orbital moments (L_z) of the Fe atoms in Fe_n ($n=2,\ldots,9$) chains at the Cu(111) surface with a magnetization pointing normal to the surface (∇, on top; $\triangle$, layer S; $\diamond$, layer S-1; $\square$, layer S-2; $\bigcirc$, in bulk; see Fig. 1).

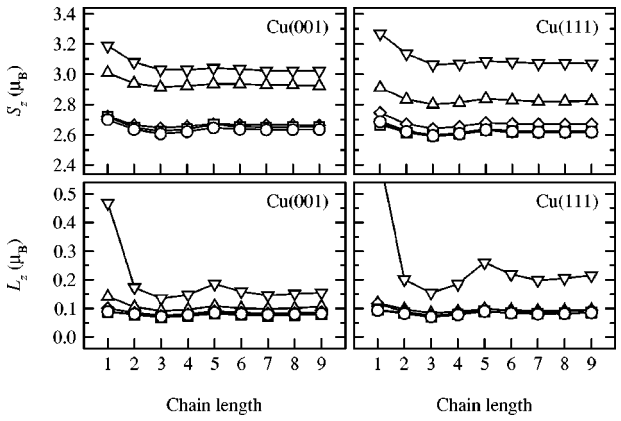

FIG. 7. Calculated spin (S_z) and orbital moments (L_z) of the central (most symmetric) Fe atom in Fe_n ($n=2,\ldots,9$) chains along the $(1\bar{1}0)$ direction at the Cu(001) and Cu(111) surfaces with a magnetization pointing normal to the surface (∇, on top; $\triangle$, layer S; $\diamond$, layer S-1; $\square$, layer S-2; $\bigcirc$, in bulk; see Fig. 1).

the corresponding Fe impurities (i.e., for the 0D case) and, in case of a Cu(001) surface, those for the corresponding monolayers (2D).[25] Thus, a systematic trend of the reduction of both S_z and L_z can be seen when increasing the dimensionality of the magnetic nanostructure, $0D \rightarrow 1D \rightarrow 2D$. A similar trend has been explored experimentally[28] and theoretically[10,24] also for Co nanostructures. Our estimated values of L_z for infinite monoatomic chains on top ($0.22\mu_B$) and in the surface layer ($0.10\mu_B$) of Cu(111) fit well into the tendency of the experimental values when reducing the thickness of the Fe film as reported in Refs. 16 and 29.

The experimental value approximated to the wire case ($\sim 0.13\mu_B$) lies between the two above calculated values of L_z, most possibly since the step-edge geometry used in the experiments can be regarded as a crossover between wires on top of the surface and those embedded into the surface layer.

IV. MAGNETIC ANISOTROPY

In Fig. 8 the MAE ΔE_{x-z} of single Fe impurities in different positions with respect to the Cu(001) and Cu(111) surfaces and the corresponding orbital moment anisotropies ΔL_{x-z} are shown. Similar to our previous observations[17,24] the spin moments of the magnetic impurities are fairly insensitive to the orientation of the effective field. Comparing Figs. 1 and 8 one can find that the orbital moment and the anisotropy of orbital moment are of the same order of magnitude, indicating that the orbital moment is indeed very sensitive to the magnetization direction coupled to the crystal due to the spin-orbit interaction. For an adatom placed on top of both kinds of surfaces an easy magnetization axis pointing perpendicular to the surface is favored, as can be inferred from the positive sign of the MAE [2.86 meV on Cu(001) and 4.30 meV on Cu(111)].

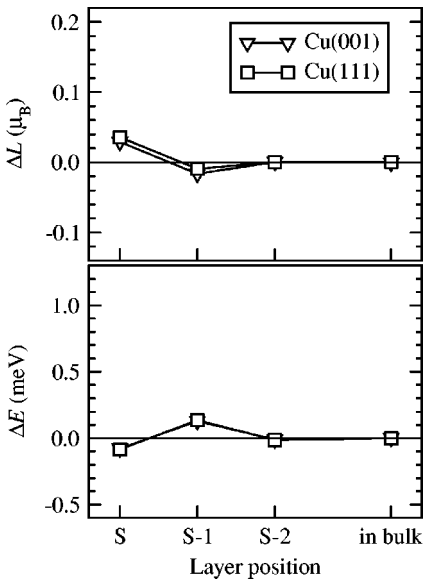

FIG. 8. Calculated orbital moment anisotropy ($\Delta L = L_x - L_z$) and magnetic anisotropy energy ($\Delta E = E_x - E_z$) of a single Fe impurity embedded at different distances from a Cu(001) and a Cu(111) surface. For the notation of the position of the impurity see Fig. 1.

TABLE I. Calculated spin moment (S_z) and orbital moment (L_z), in units of μ_B, of an Fe atom as a single impurity (0D) and in an infinite wire (1D) as estimated from the calculations for finite chains embedded along the $(1\bar{1}0)$ direction at different distances from a Cu(001) and a Cu(111) surface (on top, first vacuum layer; S, surface layer; S-1, first subsurface layer; S-2, second subsurface layer; in bulk, perfect bulk host); see also Fig. 7. For a comparison the moments of Fe in a $Cu_mFe_1Cu(001)$ overlayer system (Ref. 25) denoted by subscript 2D, are also presented by using the mapping $m=0$, on top; $m=1$, layer S-1; $m=2$, layer S-2; and $m=\infty$, in bulk.

	Cu(001)						Cu(111)			
	S_z^{0D}	S_z^{1D}	S_z^{2D}	L_z^{0D}	L_z^{1D}	L_z^{2D}	S_z^{0D}	S_z^{1D}	L_z^{0D}	L_z^{1D}
On top	3.19	3.02	2.78	0.47	0.16	0.08	3.27	3.07	0.65	0.22
S	3.01	2.92	-	0.14	0.11	-	2.91	2.82	0.12	0.10
S-1	2.72	2.66	2.61	0.10	0.09	0.07	2.74	2.67	0.12	0.09
S-2	2.72	2.65	2.58	0.09	0.08	0.06	2.67	2.62	0.10	0.09
In bulk	2.70	2.62	2.54	0.09	0.08	0.07	2.69	2.62	0.09	0.08

Remarkably, the MAE of the Fe adatom on Cu(001) is about 20 times larger as compared to the corresponding Fe monolayer case.[25] Comparing the upper and lower panels of Fig. 8 a strong correlation between ΔL and ΔE can be explored: in accordance with the qualitative rule obtained from perturbation theory[30,31] the easy axis corresponds to a maximum of the orbital moment. Clearly, both ΔL and ΔE of the Fe impurity decrease dramatically in magnitude when placed into the surface layer or below; ΔE approaches rapidly the practically vanishing MAE of the impurity embedded into the bulk with perfect cubic symmetry. As can be seen from the oscillating sign of the MAE the orientation of the easy magnetization axis depends on the distance from the surface.

Previous theoretical studies by Szunyogh and Győrffy[32] for Fe impurities buried by a Au surface also explored an oscillatory behavior of the easy axis with varying distance from the surface. As can be seen in Fig. 2 the DOS of the Fe impurity refers to the case of a completely filled majority *d* band. Thus, the most important condition to use perturbation theory *in simple terms*—namely, omitting spin-flip

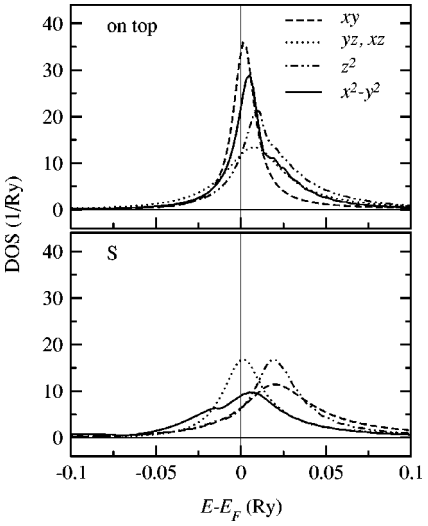

FIG. 9. Calculated *d*-like minority DOS as projected onto d_{xz}, d_{yz}, d_{xy}, d_{z^2}, and $d_{x^2-y^2}$ orbitals of a single Fe impurity deposited on (upper panel) and embedded into the surface layer (lower panel) of a Cu(001) surface.

processes—can be assumed.[30,31,33] In order to illustrate the change of the reorientation of the easy axis in terms of the electronic structure, we plotted in Fig. 9 the minority-spin DOS of an Fe adatom on Cu(001) as well as that in the surface layer as projected onto "canonical" d_α orbitals ($\alpha = xy$, xz, yz, z^2, and x^2-y^2). Note that only in this case did we "switch off" the spin-orbit coupling (SOC) using the scaling scheme proposed by Ebert *et al.*[34]

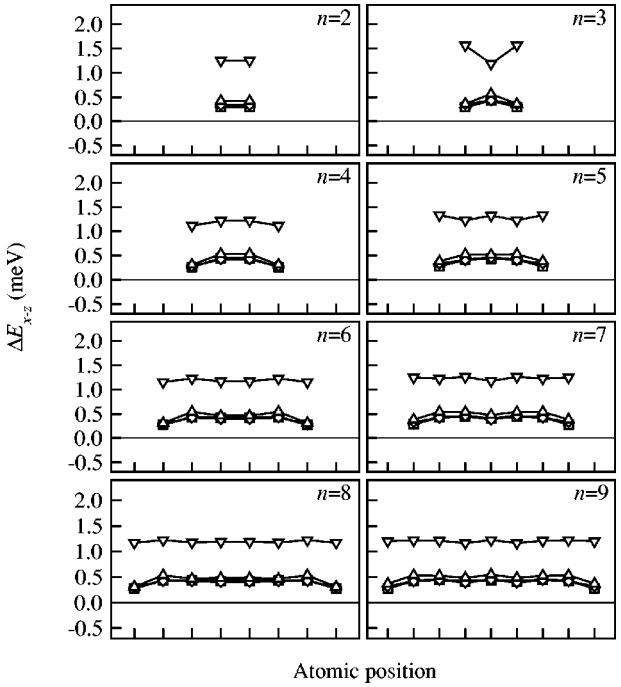

FIG. 10. Calculated contributions of Fe atoms in chains immersed at different distances from a Cu(001) surface to the magnetic anisotropy energy, ΔE_{x-z} (∇, on top; $\triangle$, layer S; $\diamond$, layer S-1; $\square$, layer S-2; $\bigcirc$, in bulk; see Fig. 1).

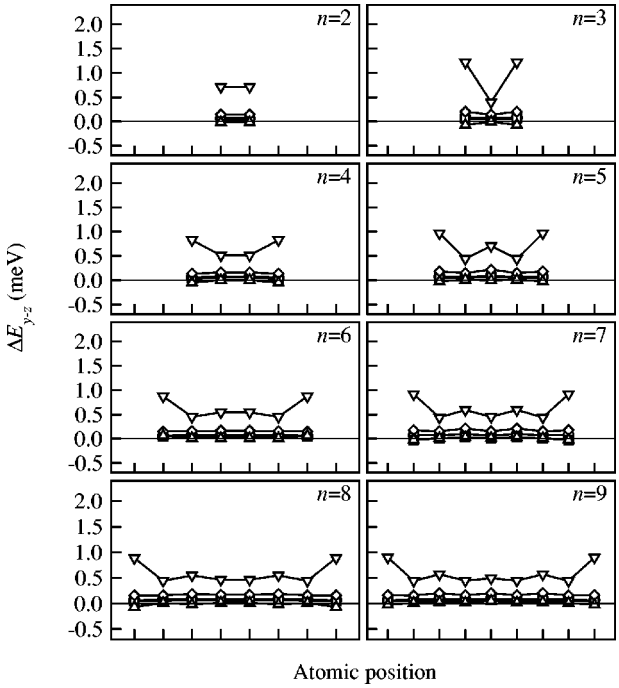

FIG. 11. Calculated contributions of Fe atoms in chains immersed at different distances from a Cu(001) surface to the magnetic anisotropy energy, ΔE_{y-z} (∇, on top; $\triangle$, layer S; $\diamond$, layer S-1; $\square$, layer S-2; $\bigcirc$, in bulk; see Fig. 1).

As can be inferred from Fig. 9, for an Fe adatom, the large d_{xy}- and $d_{x^2-y^2}$-like DOS at the Fermi level indicate a strong perpendicular anisotropy due to the interaction induced by the SOC (L_z coupling).[35] When placed into the surface layer, the in-plane states—namely, the d_{xy}- and $d_{x^2-y^2}$-like states of the impurity—get hybridized with mostly *sp*-like states of the adjacent Cu atoms, resulting in a broadening and, consequently, in a corresponding lowering of these components of the DOS at the Fermi level.

The contributions of individual Fe atoms within the chains ($n \geqslant 2$) to the MAE $\Delta E_{x-z}^{Fe_i}$ and $\Delta E_{y-z}^{Fe_i}$ ($i = 1, \ldots, n$) are displayed in Figs. 10 and 11 for a Cu(001) and in Figs. 12 and 13 for a Cu(111) surface. The first thing to note is that, although considerably decreased in magnitude as compared to the chains on top of the surfaces, all the contributions of $\Delta E_{x-z}^{Fe_i}$ remain positive for all the embedded chains; thus the orientation normal to the planes is always preferred with respect to the one along the chains. As this observation does not apply for the case of a single Fe impurity (see Fig. 8), we can conclude that the origin of an easy axis normal to the chains can be attributed to the Fe-Fe bonds along the chains.[12,36]

For chains deposited onto the surface the direction normal to planes remains the easy axis as can be inferred from the corresponding positive values of $\Delta E_{y-z}^{Fe_i}$ in Figs. 11 and 13. However, for the embedded chains the energetical difference between the two orientations normal to the chains—namely, *z* and *y*—gets very small and converges to a value below 0.1 meV/Fe atom for the chains embedded into a perfect bulk.

On top of the surfaces, for shorter chains ($n \leqslant 5$) typically

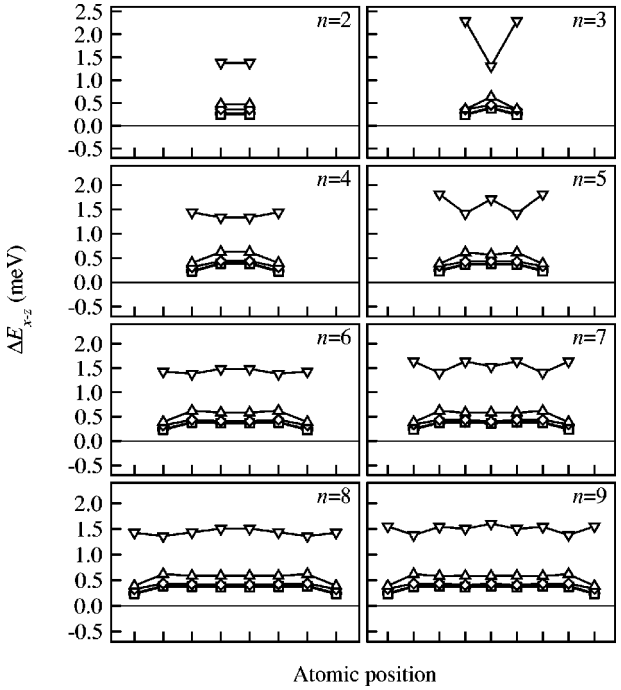

FIG. 12. Calculated contributions of Fe atoms in chains immersed at different distances from a Cu(111) surface to the magnetic anisotropy energy, ΔE_{x-z} (∇, on top; $\triangle$, layer S; $\diamond$, layer S-1; $\square$, layer S-2; $\bigcirc$, in bulk; see Fig. 1).

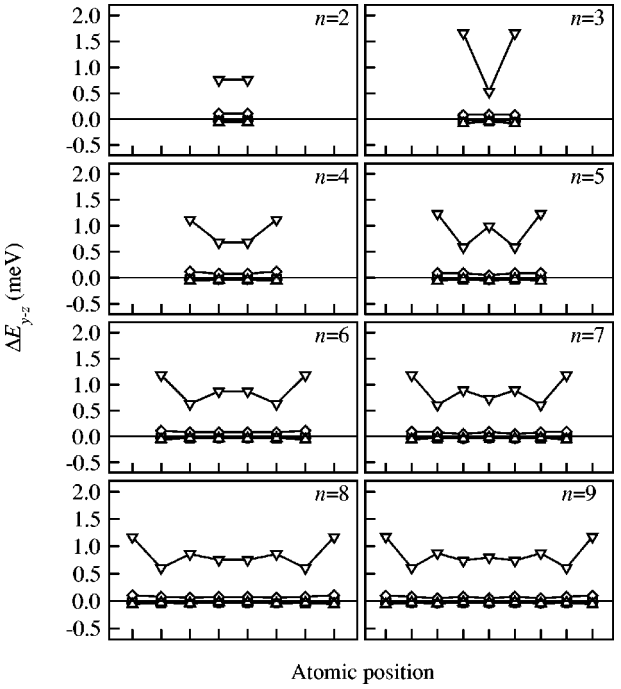

FIG. 13. Calculated contributions of Fe atoms within the chains immersed at different distances from a Cu(111) surface to the magnetic anisotropy energy, ΔE_{y-z} (∇, on top; $\triangle$, layer S; $\diamond$, layer S-1; $\square$, layer S-2; $\bigcirc$, in bulk; see Fig. 1).

rapid variations of ΔE^{Fe_i} along the chains apply. For longer chains ($n \geqslant 6$) one can find that the largest contributions to ΔE_{y-z} come from the outermost atoms, while to ΔE_{x-z} the inner and outermost sites add nearly the same contribution. Interestingly, this relationship is reversed for chains immersed in or below the surface: $\Delta E_{x-z}^{Fe_i}$ is systematically smaller at the edges of the chains than in the interior region, while $\Delta E_{y-z}^{Fe_i}$ seems to be quite homogeneous along the chains.

Except for chains on top of the surfaces, the *total MAE* of the chains (including the contributions also from the first shell of Cu sites and as normalized to one Fe atom) is shown in Fig. 14. One can immediately recognize the different behavior of ΔE_{x-z} and ΔE_{y-z} with respect to the distance from the surface: the sign of ΔE_{x-z} does not change for any embedding depth, while ΔE_{y-z} is negative for wires embedded into the first layer of a Cu(001) surface or into the first and third layers of a Cu(111) surface. Consequently, $\Delta E_{y-z} < 0$ refers to cases for which the easy axis is normal to both the surface and chain.

For chains embedded into the bulk, we obtained an easy axis perpendicular to both the (111) and $(1\bar{1}0)$ directions; i.e., it can be identified by the $(11\bar{2})$ direction. Clearly, the convergence of the total MAE with respect to the length of chains is slower than that of the spin and orbital moments of the central atoms (see Fig. 7). An approximate value for infinite wires can, however, be estimated from the data contained in Fig. 14. Similar to the orbital moment, our estimated values of ΔE_{x-z} for the infinite wires on top and embedded into the surface layer of a Cu(111) surface, ~ 1.5 meV and ~ 0.65 meV, respectively, are again in good agreement with that deduced from the experiments, ~ 1.6 meV.[16] The perpendicular MAE numerically estimated from our results for an infinite Fe wire along the (110) direction in an fcc Cu bulk host is about 0.4–0.5 meV which is approximately 3–4 times larger as obtained by Eisenbach *et al.*[12]

This difference between the two theoretical results can be attributed to the different directions of the induced moments at the Cu sites adjacent the Fe atoms which was fixed to be

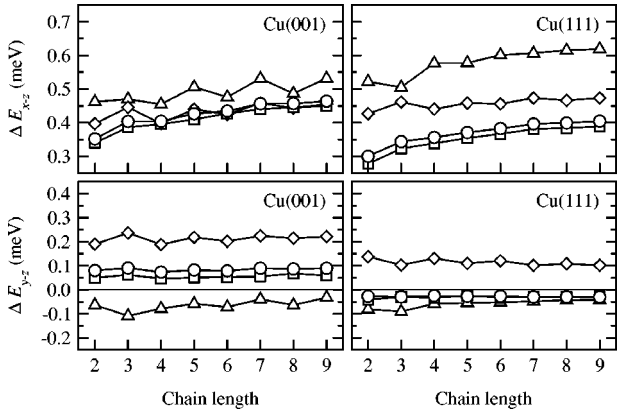

FIG. 14. Calculated magnetic anisotropy energies (MAE) ΔE_{x-z} and ΔE_{y-z} for Fe_n ($n=2,\ldots,9$) chains immersed at different distances from a Cu(111) and a Cu(001) surface including also contributions from the nearest-neighbor Cu sites and normalized to one Fe atom ($\triangle$, layer S; $\diamond$, layer S-1; $\square$, layer S-2; $\bigcirc$, in bulk; see Fig. 1).

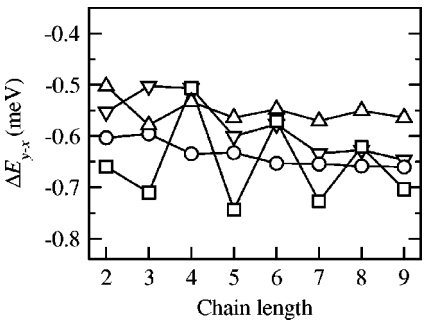

FIG. 15. Calculated in-plane magnetic anisotropy energy (MAE) ΔE_{x-y}, for Fe_n ($n=1,\ldots,9$) chains on a Cu(001) and a Cu(111) surface including also contributions from nearest-neighbor Cu sites and normalized to one Fe atom [∇, Cu(001) on top; $\triangle$, Cu(001) layer S; $\square$, Cu(111) on top; $\bigcirc$, Cu(111) layer S; see Fig. 1].

parallel to the Fe moments in our calculations but was freely fluctuating in Ref. 12. It should, however, be noted that the calculations of Ref. 12 have been performed by using periodic boundary conditions in the plane normal to the wire; therefore, the corresponding results (in particular, the MAE) can also be influenced by ''interchain'' interactions.

In Fig. 15 the *in-plane* magnetic anisotropy energies ΔE_{y-x} of chains on top and embedded into the surface layer of Cu(001) and Cu(111) surfaces are displayed with respect to the length of Fe chains. In particular, for chains on top of the Cu(111) surface, ΔE_{y-x} shows rapid oscillations (with a period of two atoms), indicating that the in-plane MAE is influenced by confinement effects caused most possibly by surface states. The extrapolated value of the in-plane MAE for an infinite chain on a Cu(111) surface, $\sim$ 0.5 meV, is very close to the experimental value of about 0.4 meV reported by Boeglin *et al.*[16]

In order to complete the comparison between our calculations and experiment we also estimated the anisotropy of the orbital moment for an infinite Fe wire from the calculated values for the sites at the center of longer chains ($n \geqslant 7$), yielding a value of $\Delta L_{y-x} \simeq 0.025\ \mu_B$ on top of a Cu(111) surface and $\Delta L_{y-x} \simeq 0.035 \mu_B$ in the corresponding surface layer, again in good agreement with the experimental data $\Delta L_{y-x} \simeq 0.032 \mu_B$ (Ref. 16).

V. CONCLUSIONS

Using a real-space embedded cluster technique based on the Korringa-Kohn-Rostoker Green function method, we carried out fully relativistic self-consistent calculations for finite Fe chains oriented along the $(1\bar{1}0)$ direction near the Cu(001) and Cu(111) surfaces. We found that the magnetic properties of the Fe chains strongly depend on the distance from the surface, i.e., on the local environment. As compared to the monolayer case, we found enhanced spin and orbital moments as well as magnetic anisotropy energies for the chains mainly controlled by the coordination of the magnetic atoms.

In the special case of a single Fe impurity, we illustrated the changes of the spin moment and MAE with respect to the position of the impurity in terms of the corresponding changes in the electronic structure. For most of the quantities under consideration we found a reasonable convergence when increasing the length of the chains. Thus, the corresponding quantities for the infinite chain (1D) could easily be estimated. Similar to our previous calculations for Co chains on Pt(111),[24] we showed that from calculations for rather short linear chains the magnetic properties for long (ideally infinite) chains can be deduced, keeping, however, the possibility to study local fluctuations (finite-size effects) within the chains. Although a different geometry was used in our calculations, the easy axis of the system and the size of the MAE as well as the orbital moment anisotropy are in good agreement with available experiments.[37]

ACKNOWLEDGMENTS

This paper resulted from a collaboration partially funded by the RTN network ''Computational Magnetoelectronics'' (Contract No. HPRN-CT-2000-00143). Financial support was also provided by the Center for Computational Materials Science (Contract No. GZ 45.451), the Austrian Science Foundation (Contract No. W004), and the Hungarian National Scientific Research Foundation Grant Nos. (OTKA T037856 and OTKA M36482), and the Research and Technological Cooperation Project between Austria and Hungary (Contract No. A-23/01).

[1] H.J. Elmers, J. Hauschild, H. Höche, U. Gradmann, H. Bethge, D. Heuer, and U. Köhler, Phys. Rev. Lett. **73**, 898 (1994).
[2] P. Gambardella, M. Blanc, H. Brune, K. Kuhnke, and K. Kern, Phys. Rev. B **61**, 2254 (2000).
[3] P. Gambardella, M. Blanc, L. Bürgi, K. Kuhnke, and K. Kern, Surf. Sci. **449**, 93 (2000).
[4] P. Gambardella, A. Dallmeyer, K. Maiti, M.C. Malagoli, W. Eberdardtan, K. Kern, and C. Carbone, Nature (London) **416**, 301 (2002).
[5] S.M. York and F.M. Leibsle, Phys. Rev. B **64**, 33411 (2001).
[6] K. Wildberger, V.S. Stepanyuk, P. Lang, R. Zeller, and P.H. Dederichs, Phys. Rev. Lett. **75**, 509 (1995).
[7] V. Bellini, N. Papanikolaou, R. Zeller, and P.H. Dederichs, Phys. Rev. B **64**, 094403 (2001).
[8] R. Družinić and W. Hübner, Phys. Rev. B **55**, 347 (1997).
[9] J. Dorantes-Dávila and G.M. Pastor, Phys. Rev. Lett. **81**, 208 (1998).
[10] M. Komelj, C. Ederer, J.W. Davenport, and M. Fähnle, Phys. Rev. B **66**, 140407 (2002).
[11] D. Spišák and J. Hafner, Phys. Rev. B **65**, 235405 (2002).
[12] M. Eisenbach, B.L. Györffy, G.M. Stocks, and B. Újfalussy, Phys. Rev. B **65**, 144424 (2002).
[13] V.S. Stepanyuk, D.V. Tsivline, D.I. Bazhanov, W. Hergert, and A.A. Katsnelson, Phys. Rev. B **63**, 235406 (2001).
[14] J. Shen, R. Skomski, M. Klaua, H. Jenniches, S.S. Manoharan, and J. Kirschner, Phys. Rev. B **56**, 2340 (1997).

[15] J. Shen, M. Klaua, P. Ohresser, H. Jenniches, J. Barthel, C.V. Mohan, and J. Kirschner, Phys. Rev. B **56**, 11 134 (1997).
[16] C. Boeglin, S. Stanescu, J.P. Deville, P. Ohresser, and N.B. Brookes, Phys. Rev. B **66**, 014439 (2002).
[17] B. Lazarovits, L. Szunyogh, and P. Weinberger, Phys. Rev. B **65**, 104441 (2002).
[18] L. Szunyogh, B. Újfalussy, P. Weinberger, and J. Kollár, Phys. Rev. B **49**, 2721 (1994).
[19] L. Szunyogh, B. Újfalussy, P. Weinberger, and J. Kollár, J. Phys.: Condens. Matter **6**, 3301 (1994).
[20] S.H. Vosko, L. Wilk, and M. Nusair, Can. J. Phys. **58**, 1200 (1980).
[21] G.H.O. Daalderop, P.J. Kelly, and M.F.H. Schuurmans, Phys. Rev. B **41**, 11 919 (1990).
[22] L. Szunyogh, B. Újfalussy, and P. Weinberger, Phys. Rev. B **51**, 9552 (1995).
[23] H.J.F. Jansen, Phys. Rev. B **59**, 4699 (1999).
[24] B. Lazarovits, L. Szunyogh, and P. Weinberger, Phys. Rev. B **67**, 024415 (2003).
[25] B. Újfalussy, L. Szunyogh, and P. Weinberger, Phys. Rev. B **54**, 9883 (1996).
[26] V.S. Stepanyuk, W. Hergert, P. Rennert, K. Wildberger, R. Zeller, and P.H. Dederichs, Surf. Sci. **377-379**, 495 (1997).
[27] J.B. Staunton, B.L. Györffy, J. Poulter, and P. Strange, J. Phys. C **21**, 1595 (1988).
[28] P. Poulopoulos and K. Baberschke, J. Phys.: Condens. Matter **11**, 9495 (1999).
[29] P. Ohresser, G. Ghiringhelli, O. Tjernberg, N.B. Brookes, and M. Finazzi, Phys. Rev. B **62**, 5803 (2000).
[30] P. Bruno, Phys. Rev. B **39**, 865 (1989).
[31] G. van der Laan, J. Phys.: Condens. Matter **10**, 3239 (1998).
[32] L. Szunyogh and B.L. Györffy, Phys. Rev. Lett. **78**, 3765 (1997).
[33] J. Stöhr, J. Magn. Magn. Mater. **200**, 470 (1999).
[34] H. Ebert, H. Freyer, A. Vernes, and G.Y. Guo, Phys. Rev. B **53**, 7721 (1996).
[35] J. Stöhr and H. König, Phys. Rev. Lett. **75**, 3748 (1995).
[36] D. Wang, R. Wu, and A.J. Freeman, Phys. Rev. B **47**, 14 932 (1993).
[37] A.B. Klautau and S. Frota-Pessôa, Surf. Sci. **497**, 385 (2001).